



UNIVERSITY OF LEEDS

This is a repository copy of *Miniaturized dielectric waveguide filters*.

White Rose Research Online URL for this paper:
<http://eprints.whiterose.ac.uk/88315/>

Version: Accepted Version

Article:

Sandhu, MY orcid.org/0000-0003-3081-8834 and Hunter, IC
orcid.org/0000-0002-4246-6971 (2016) Miniaturized dielectric waveguide filters.
International Journal of Electronics, 103 (10). pp. 1776-1787. ISSN 0020-7217

<https://doi.org/10.1080/00207217.2016.1138531>

Reuse

Unless indicated otherwise, fulltext items are protected by copyright with all rights reserved. The copyright exception in section 29 of the Copyright, Designs and Patents Act 1988 allows the making of a single copy solely for the purpose of non-commercial research or private study within the limits of fair dealing. The publisher or other rights-holder may allow further reproduction and re-use of this version - refer to the White Rose Research Online record for this item. Where records identify the publisher as the copyright holder, users can verify any specific terms of use on the publisher's website.

Takedown

If you consider content in White Rose Research Online to be in breach of UK law, please notify us by emailing eprints@whiterose.ac.uk including the URL of the record and the reason for the withdrawal request.



eprints@whiterose.ac.uk
<https://eprints.whiterose.ac.uk/>

Miniaturized Dielectric Waveguide Filters

Muhammad Y Sandhu*, Ian C Hunter**

Institute of Microwave & Photonics, University of Leeds, Woodhouse Lane, LS2 9JT,
Leeds, UK

*M.Y.Sandhu@leeds.ac.uk

**I.C.Hunter@leeds.ac.uk

Miniaturized Dielectric Waveguide Filters

Design techniques for a new class of integrated monolithic high permittivity ceramic waveguide filters are presented. These filters enable a size reduction of 50% compared to air-filled TEM filters with the same unloaded Q-Factor. Designs for chebyshev and asymmetric generalized chebyshev filter and a diplexer are presented, with experimental results for an 1800 MHz chebyshev filter and a 1700 MHz generalized chebyshev filter showing excellent agreement with theory.

Keywords: Microwave filter; ceramic filter; dielectric waveguide filter; integrated waveguide filter; ceramic bandpass filter

1. Introduction

Cellular radio base stations routinely use TEM filters and multiplexers. These filters are relatively simple to manufacture and offer high Q and good spurious performance, although they use significant physical volume (Atia, Williams et al. 1974). There is significant pressure for future systems to increase the number of filters and consequently a reduction in size without compromising electrical performance is required. A survey of most often used techniques in microwave filter design is presented by Levy (Levy, Snyder et al. 2002). Dielectric resonator filters were first introduced by Cohn in 1968 using the dielectric material titanium dioxide (TiO₂) of relative permittivity 100 and loss tangent 0.0001 (Cohn 1968). Dielectric materials are evaluated based on their relative permittivity, temperature coefficient and Q value due to dielectric loss (Nishikawa 1988). A compact dielectric filled waveguide band pass filter operating at X-band (8-12 GHz) is reported by Ghorbaninejad (Khalaj-Amirhosseini 2008). A monolithic multiple dielectric loaded waveguide filter is designed by Kapilevich (Kapilevich and Trubekhin 1989).

In this paper, we present new designs for ceramic filled rectangular waveguide filters. These filters offer for a given unloaded Q a reduction in size of 50% or more. The filters consist of mono-blocks of high permittivity ceramic with various through and blind holes to realize the complex inter-resonator couplings for both in-line and cross coupled filters. The exterior surface is metallized with conductive ink. Experimental results are presented for a Chebyshev and a generalized Chebyshev design with an EM simulation

of more complex diplexer.

2. Ceramic Waveguide Resonator

Consider the resonator shown in Figure 1 (iii), consisting of a solid rectangular block of high permittivity ceramic, with the exterior metalized. The resonant frequency and Q-Factor of waveguide modes are readily computed from (Matthaei 1980). For the fundamental TE₁₀ mode, as the dielectric constant is increased then the physical dimensions and unloaded Q decrease by a factor of $\frac{1}{\sqrt{\epsilon_r}}$ (Sebastian 2008).

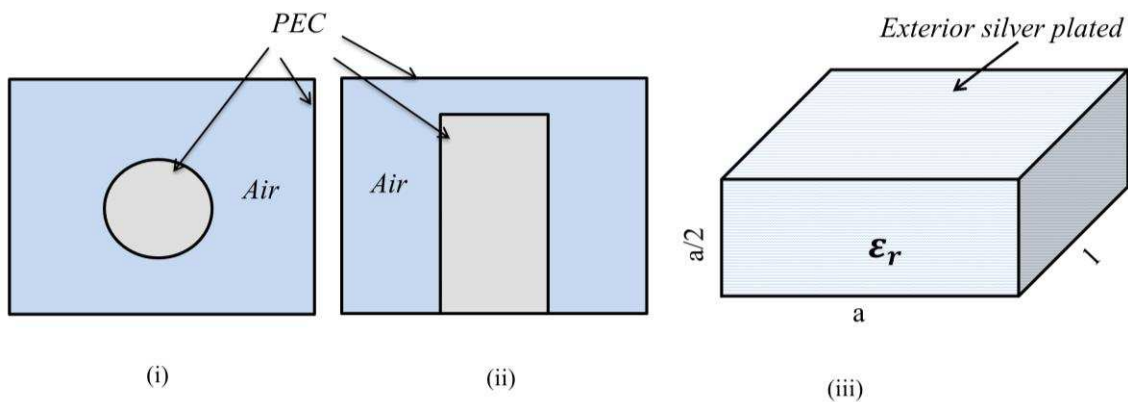


Figure 1 (i) Coaxial Resonator Top View (ii) Coaxial resonator Side View (iii) Ceramic waveguide resonator

A numerical simulation of a comparison between an air filled coaxial resonator (Figure 1) and the ceramic waveguide resonator for a resonant frequency of 1GHz is shown in Figure 2. This demonstrates that the dielectric waveguide offers a potential size reduction of 50% or more when compared with air- filled coaxial comb-line resonators with the same Q-Factor.

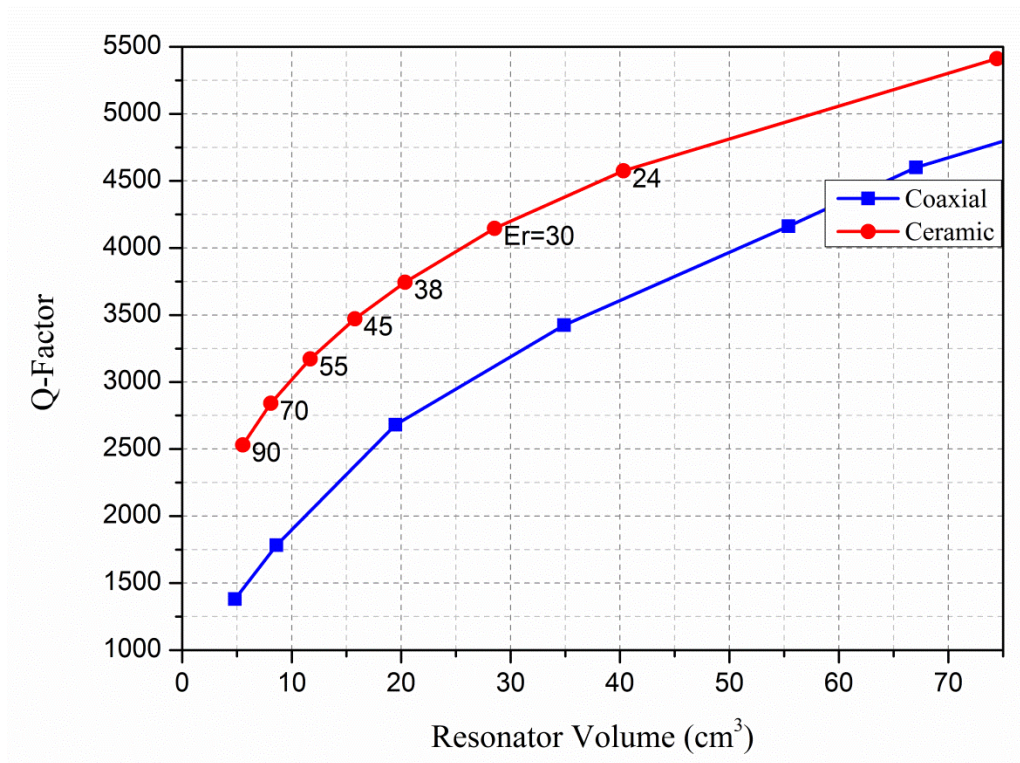


Figure 2 Q vs Volume comparison between comb-line coaxial and ceramic waveguide resonator at 1GHz

3. Chebyshev Filter Realization

A six pole ceramic waveguide filter with the following specification was designed using $\lambda g/2$ resonators separated by metalized holes in ceramic.

- Centre frequency : 1842MHz
- Bandwidth : 75MHz
- Ceramic Permittivity : 45

The filter consists of a silver plated rectangular ceramic bar with various through holes. The holes provide inductive inter-resonator couplings and the design technique described in (Hunter 2001) may be used. Adjustment in inverter susceptance can be achieved with fixed number of holes of fixed diameter by varying the distance among them (Marcuvitz and Engineers 1951). Inductive holes are placed symmetrically across the waveguide broad dimension in order to suppress the higher order modes. The equivalent circuit of a six pole Chebyshev ceramic waveguide filter is shown in Figure 3.

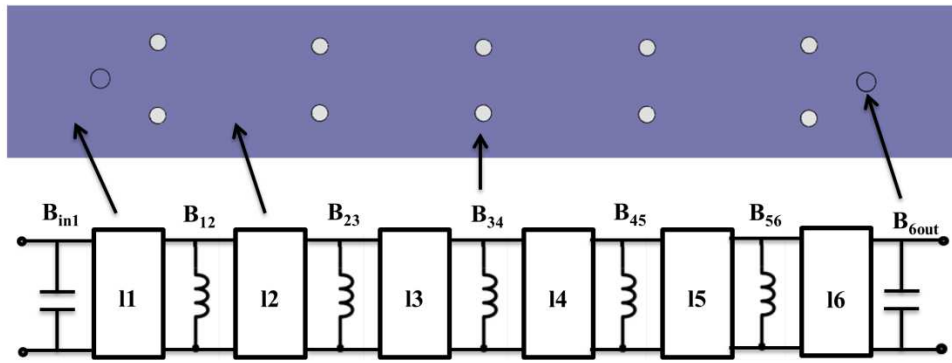


Figure 3 Six pole ceramic waveguide filter equivalent circuit

The structure is silver plated except for the input /output coupling probe positions. Input /output coupling is achieved using coaxial probes. The probe position from the shorted back end, diameter and depth inside the waveguide determine the amount of coupling achieved, bandwidth and centre frequency. Comparison of HFSS simulation and measured filter response is given in Figure 4.

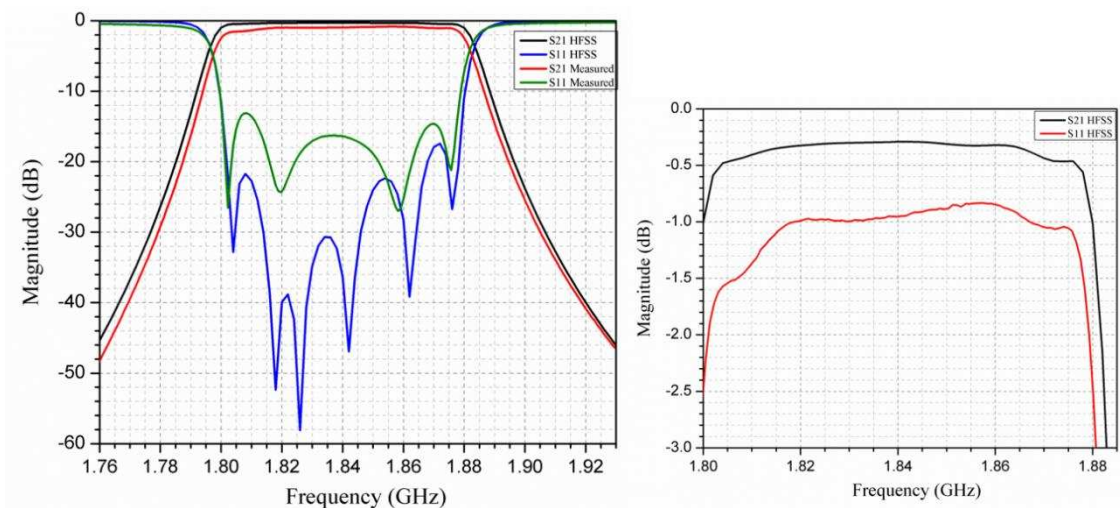


Figure 4 Six pole Chebyshev filter measured vs HFSS simulated response without tuning screws

Simulations give a resonator Q-factor of 2400 however the measured pass band insertion loss was higher than the simulated loss. This was mainly due to leakage at the input and output and also slightly due to reflection, as there were no tuning screws in the filter. This is being corrected in future designs. A photograph of the fabricated filter is shown in Figure 5.

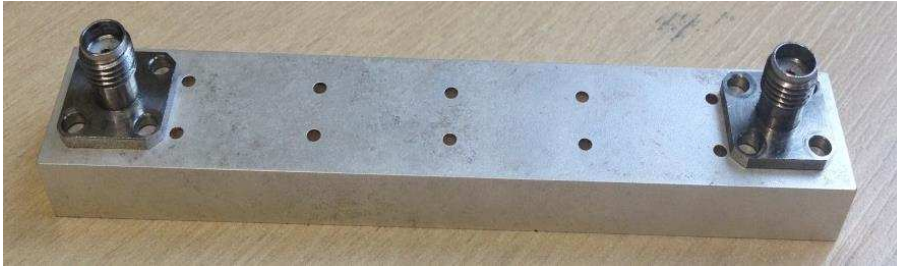


Figure 5. Fabricated six pole Chebyshev ceramic waveguide filter

4. Generalized Chebyshev Ceramic Waveguide Filter

A more complex design of a six section cross coupled ceramic waveguide filter operating at DCS uplink frequency was designed using two cross coupled triplets to meet the following specifications.

Centre frequency	1730MHz
Bandwidth	60MHz
Ceramic Permittivity	43
Rejection	80 dB at $f < 1645\text{MHz}$
	80 dB at $f > 1845\text{MHz}$

Achieving higher out of band rejection with a lower number of elements is possible by introducing finite frequency transmission zeros. There are several methods in the literature to introduce transmission zeros in a waveguide band pass filter e.g. by cross couplings between non-adjacent resonators (Atia, Williams et al. 1974; Levy and Petre 2001) or by introducing suitable parasitic resonators in the filter (Rhodes and Cameron 1980; Cameron 2003; Sorrentino, Pelliccia et al. 2011). A finite frequency transmission zero is produced due to the destructive interference of multipath (direct and cross coupled) in a cross coupled arrangement (Thomas 2003). Kurzrok (Kurzrok 1966; Kurzrok 1966) introduced cross coupled triplet and quadruplet in waveguide band pass filter in the early stages of microwave filter designs. The coupling matrix for the generalized Chebyshev filter was derived with the method described in (Cameron 1999) and is given below.

	S	1	2	3	4	5	6	L
S	0	1.0626	0	0	0	0	0	0
1	1.0626	-0.0035	0.8897	0.1218	0	0	0	0
2	0	0.8897	-0.1749	0.6232	0	0	0	0
3	0	0.1218	0.6232	0.0101	0.5993	0	0	0
4	0	0	0	0.5993	-0.0341	0.6097	-0.1969	0
5	0	0	0	0	0.6097	0.2713	0.8761	0
6	0	0	0	0	-0.1969	0.8761	-0.0035	1.0626
L	0	0	0	0	0	0	1.0626	0

A transmission zero at the high side of pass band is produced by introducing an inductive cross coupled triplet to achieve specified out of band rejection level. In a ceramic waveguide filter all positive cross couplings can be achieved by metal plated through holes. The position of transmission zero above the pass band can be controlled by varying the cross coupling across non-adjacent resonators i.e. varying the distance and radius of through holes placed between cross coupled resonators. The stronger is the cross coupling, the closer is the transmission zero to the pass band. The transmission zero at the lower side of the passband is produced by introducing a capacitive cross coupled triplet. The capacitive cross coupling is achieved by placing a metal plated blind hole at the centre of the broad wall of the waveguide between cross-coupled resonators as shown in Figure 6.

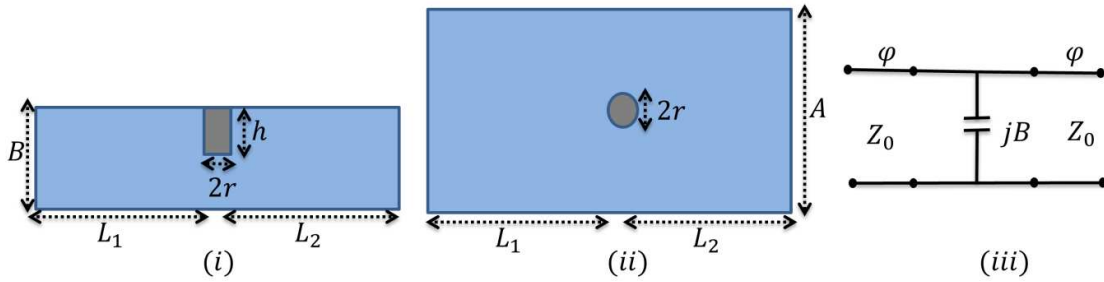


Figure 6: Waveguide capacitive impedance inverter (i) Side view (ii) Top view (iii) Equivalent circuit

The transfer matrix of the capacitive shunt discontinuity embedded in a uniform length of waveguide with electrical length Ψ , can be written as

$$[T] = \begin{bmatrix} \cos\Psi & j\sin\Psi \\ j\sin\Psi & \cos\Psi \end{bmatrix} \begin{bmatrix} 1 & 0 \\ jB & 1 \end{bmatrix} \begin{bmatrix} \cos\Psi & j\sin\Psi \\ j\sin\Psi & \cos\Psi \end{bmatrix}$$

$$= \begin{bmatrix} \cos^2 \Psi - B \cos \Psi \sin \Psi - \sin^2 \Psi & j \sin \Psi [2 \cos \Psi - B \sin \Psi] \\ j \cos \Psi [2 \sin \Psi + B \cos \Psi] & \cos^2 \Psi - B \cos \Psi \sin \Psi - \sin^2 \Psi \end{bmatrix} \quad (1)$$

In an ideal shunt capacitive impedance inverter transfer matrix $A_{ABCD} = D_{ABCD} = 0$, therefore

$$\cos^2 \Psi - B \cos \Psi \sin \Psi - \sin^2 \Psi = 0 \quad (2)$$

$$\Rightarrow \cos^2 \Psi - \sin^2 \Psi = B \cos \Psi \sin \Psi$$

$$\Rightarrow \cos 2\Psi = \frac{B \sin 2\Psi}{2}$$

$$\Rightarrow \cos 2\Psi = B \sin 2\Psi$$

$$\Rightarrow B = 2 \cot(2\Psi) \quad (3)$$

Also by comparing transfer matrix to an ideal shunt capacitor transfer matrix

$$jK = j \cos \Psi [2 \sin \Psi + B \cos \Psi] \quad (4)$$

$$\Rightarrow K = \cos \Psi [2 \sin \Psi + B \cos \Psi]$$

$$\Rightarrow K = 2 \cos \Psi \sin \Psi + B \cos^2 \Psi \quad (5)$$

From trigonometric identity

$$\cos^2 \Psi = \frac{1 + \cos(2\Psi)}{2} \quad \text{and} \quad 2 \cos \Psi \sin \Psi = \sin(2\Psi)$$

Therefore by putting in (5)

$$K = \sin(2\Psi) + B \frac{1 + \cos(2\Psi)}{2}$$

$$K = \sin(2\Psi) + 2 \cot(2\Psi) \frac{1 + \cos(2\Psi)}{2}$$

$$K = \sin(2\Psi) + \cot(2\Psi) + \cot(2\Psi)\cos(2\Psi)$$

$$K = \sin(2\Psi) + \cos(2\Psi)/\sin(2\Psi) + \cos^2(2\Psi)/\sin(2\Psi)$$

$$k = [1 + \cos(2\Psi)]/\sin(2\Psi)$$

$$k = 2 \cos^2(\Psi) / 2 \sin(\Psi) \cos(\Psi) \quad (6)$$

$$k = \cot(\Psi) \quad (7)$$

Now from eq:(3) $B = 2\cot(2\Psi)$

But $\cot(2\Psi) = [1 - \tan^2(\Psi)] / 2\tan\Psi \quad (8)$

$$B = 2[1 - \tan^2(\Psi)] / 2\tan\Psi$$

Put $\tan\Psi = 1/\cot\Psi = 1/k$, Thus

$$B = \left[1 - \frac{1}{k^2}\right] / 1/k$$

$$B = [k^2 - 1]/k \quad (9)$$

$$\text{As } |k| < 1 \Rightarrow k < 0$$

This metal plated blind hole behaves as a frequency dependent resonating structure. Therefore, besides providing capacitive cross coupling it resonates at a higher frequency and it produces another transmission zero. The position of this extra transmission zero can be moved away from the passband by selecting the proper diameter of the blind hole. The input and output couplings are achieved by 50 ohm coaxial probes. The Probe diameter, depth inside the waveguide, its distance from the shorted backend and offset from centre determines its coupling bandwidth, power handling and centre frequency (Liang, Chang et al. 1992). Figure 7 shows the final layout and the fabricated filter hardware of the cross coupled generalized Chebyshev filter designed to operate at DCS uplink frequency band.

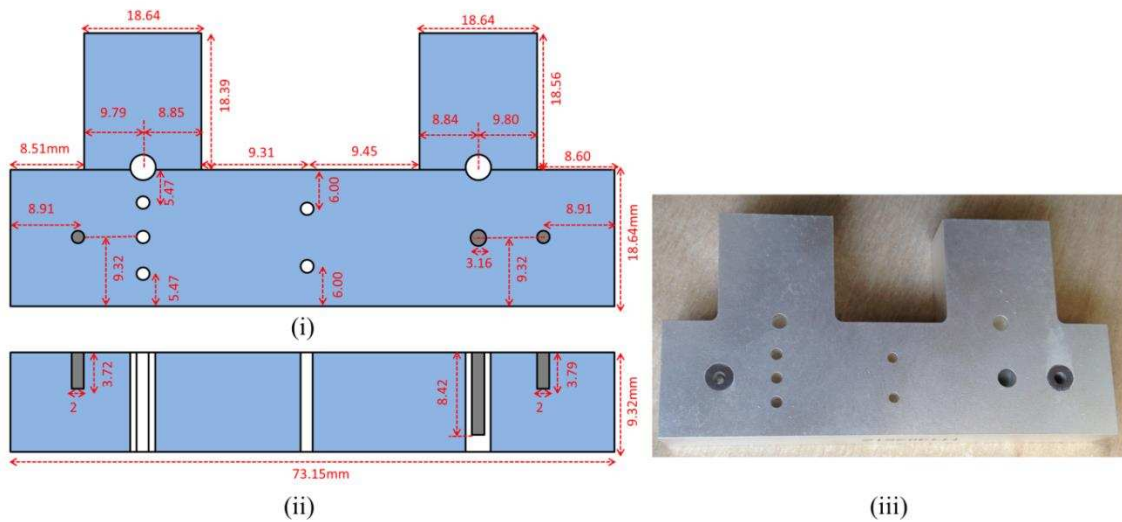


Figure 7 Generalized Chebyshev Cross Coupled Ceramic Waveguide Filter (i) Top view (ii) Cross sectional view (iii) Hardware

Figure 8 shows the comparison of HFSS simulated and measured S-parameters of a six section cross coupled ceramic waveguide filter without tuning screws. Measurement shows that bandwidth of the passband is increased, the overall passband is shifted to the lower side and a severe mismatch occurs at the higher side of the passband. This is due to the presence of curved radii of side resonators in the physical design, which are not included in the EM simulations. Also the lower side transmission zero is moved further away from passband, due to change in resonance and coupling bandwidth of the side resonators of the filter. The high side transmission zero is not clearly visible in measured response as it is buried in the noise floor. The passband insertion loss is about 0.7 dB in the region of passband where filter is well matched. The next design with tuning screws includes the curved radii of side resonators in EM simulation.

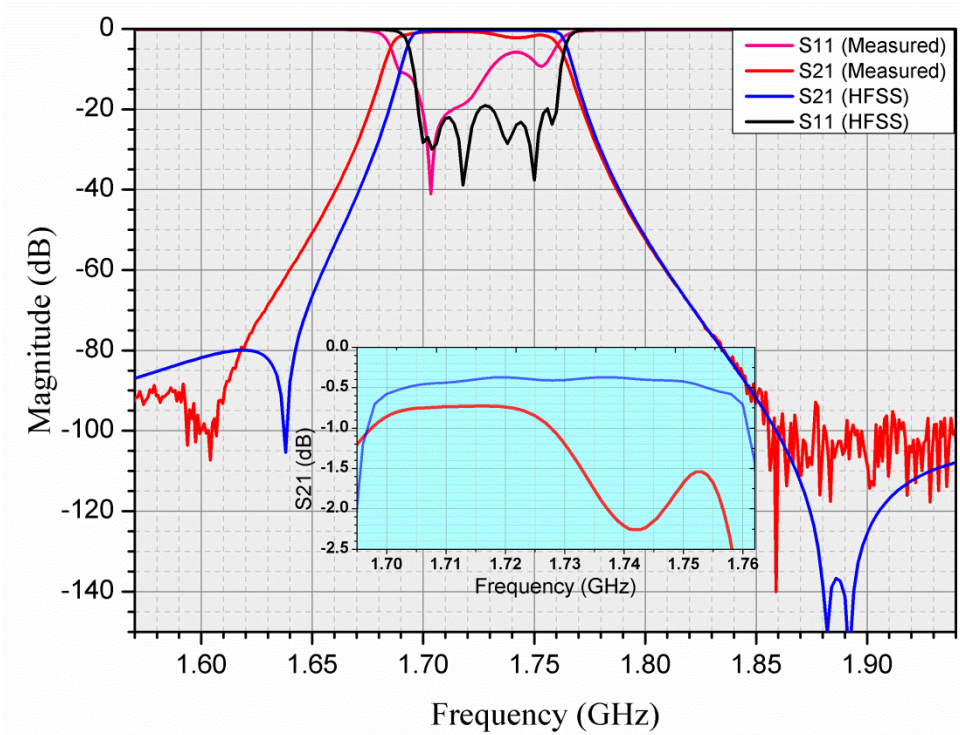


Figure 8. Generalized Chebyshev ceramic waveguide simulated and measured filter response (HFSSTM)

5. Generalized Chebyshev filter with tuning screws

The measured response of Chebyshev ceramic waveguide filter designed in section.4 needs tuning to mitigate the effects of material discrepancies and physical dimension tolerances. The silver tuning screws are placed at the bottom broad wall of the filter in each resonator section to compensate discrepancies in the fabricated filter. Tuning screws are placed at the centre of the each resonator to perturb maximum E-field region of resonator except first and last resonator section, where tuning screws are placed midway between centre of the broad wall and side wall so as to keep input coupling unaffected when tuning resonance of the resonator. The waveguide filter is simulated with tuning screws half way inside the tuning hole, so as to keep the option of both way post production tuning mechanism. The fabricated generalized Chebyshev ceramic waveguide filter having transmission zeros at above and below the pass band and with tuning screws in it is shown in Figure 9.

A comparison of HFSS simulated and measured results of generalized Chebyshev ceramic waveguide filter with tuning screws is shown in Figure 10. The

measured results show an agreement with simulated S-parameters except position of low side transmission zero shifted towards passband. This is mainly due to physical tolerance of blind hole depth used to provide cross coupling between resonator 4-6.

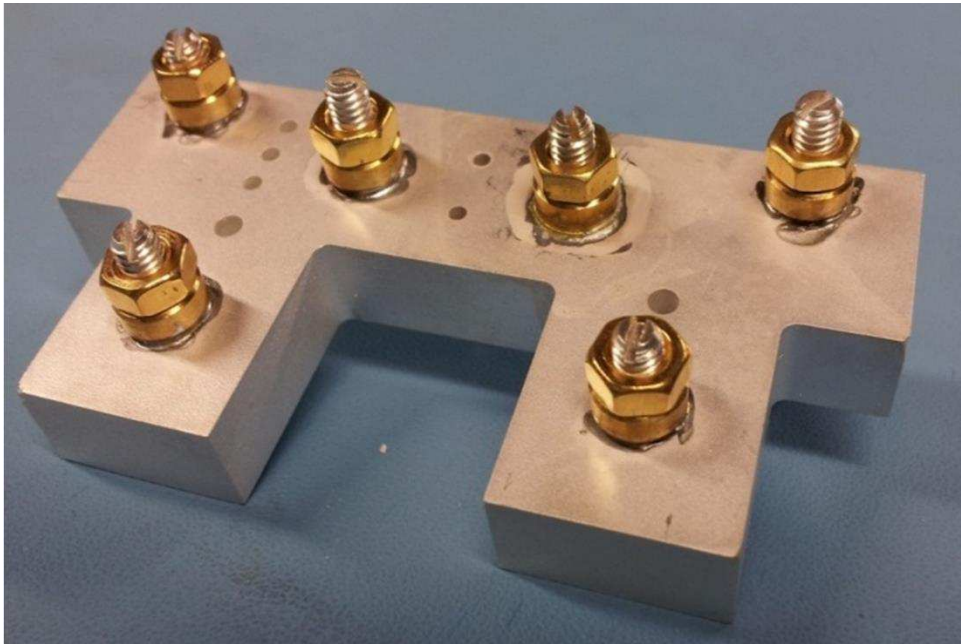


Figure 9. Fabricated generalized Chebyshev filter with tuning screws

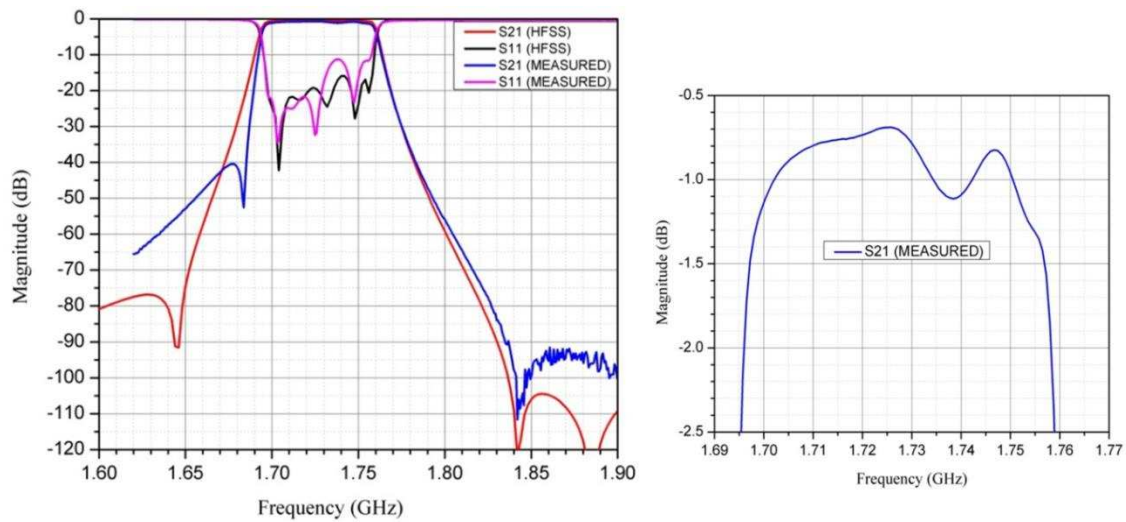


Figure 10. Simulated and measured response of generalized Chebyshev ceramic waveguide filter with tuning screws

6. Integrated Diplexer Design

A miniaturized integrated ceramic waveguide diplexer is designed for the following channel specifications.

Table 1 : Specification for diplexer

Specifications	Transmit Channel Filter	Receive Channel Filter
Passband Bandwidth	60 MHz (2100 MHz-2160 MHz)	60 MHz
Centre Frequency	2130 MHz	1730 MHz
Passband RL	> 20 dB	> 20 dB
Stopband Attenuation	>50 dB at $f < 2060$ MHz & $f > 2200$ MHz	> 70 dB at DC $< f < 1650$ MHz > 80 dB at 1880 MHz $< f < 2200$ MHz

Diplexers are essentially two channel multiplexers and can be accomplished by designing individual doubly terminated band pass filters for each branch and then connecting them in parallel (Matthaei 1980). However, interaction between two filters must be avoided by optimizing the common junction. Although there exist some exact synthesis methods to design a diplexer in the literature (Rhodes 1976; Haine and Rhodes 1977; Levy 1990; Macchiarella and Tamiazzo 2006). Yet the most common approach used to design a microwave diplexer is based on the optimization techniques (Sanghoon and Kanamaluru 2007; Wolansky, Vorek et al. 2010). If the separation between RX and TX band filters is wide enough then optimisation techniques can give satisfactory results in a very small time. Due to the loading effect, the first resonator and the input coupling bandwidths need to be slightly modified. If the centre frequencies of both filters are not too close then only a small amount of tuning is needed. Figure 11 represents the block diagram of the diplexer combining a Chebyshev (TX) bandpass filter and a generalized Chebyshev (RX) bandpass filter and its circuit simulated S-parameter response is given in Figure 12.

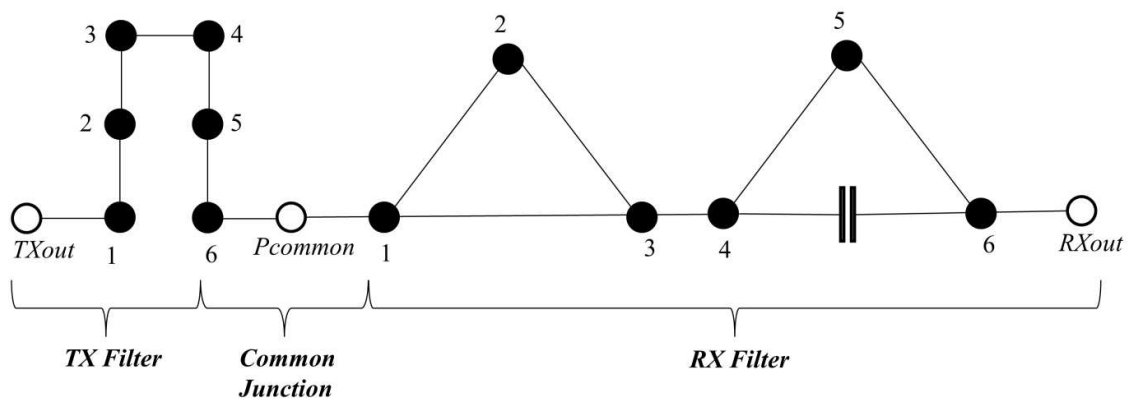


Figure 11 : Diplexer coupling scheme

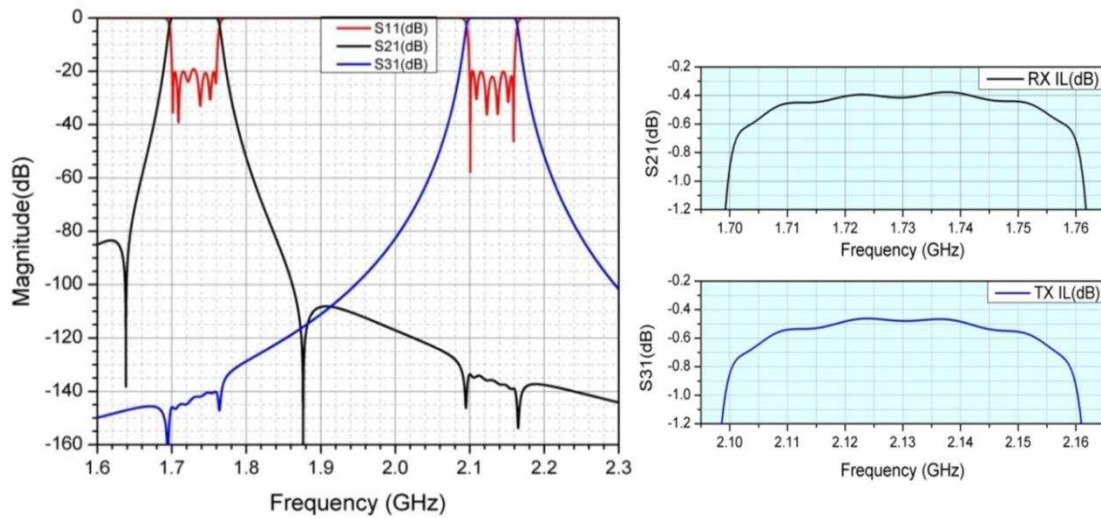


Figure 12. Circuit simulated S-parameters of diplexer

Ceramic waveguide realization

The ceramic waveguide diplexer can be designed by adding the two filters in parallel to a common junction. A T-Junction is a three port lossless reciprocal device which connects two TE₁₀ mode waveguide channel filters to the common input port (Helszajn and Engineers 2000). The phase length between input of each filter and common port determines the isolation of each filter in opposite filter pass band. The length of the common junction is needed to be optimized in order to provide isolation between outputs of the side ports. Figure 13 shows the physical layout of a monolithic integrated ceramic waveguide diplexer. Doubly terminated waveguide filters are designed first and then they are connected in parallel through a common junction. The common junction is the extra ceramic piece which sits between TX and RX filter. The common coaxial probe is placed in this junction to achieve the input couplings to both filters. Each filter section is coupled through metal plated through holes (shunt inductors) placed between common junction and each individual filter. Each filter section and the common junction are optimized individually to reduce the EM simulation time and afterwards an optimization of full diplexer was carried out using HFSSTM EM simulator. The length of the input probe inside the waveguide used at common junction is optimized to provide wideband optimal return loss in both TX and RX passband. The bandwidth of the probe is increased by moving its position from the centre of the waveguide towards the side

wall of the waveguide (Keam and Williamson 1994). Figure 14 shows the S-parameter response of the EM simulated integrated ceramic waveguide diplexer.

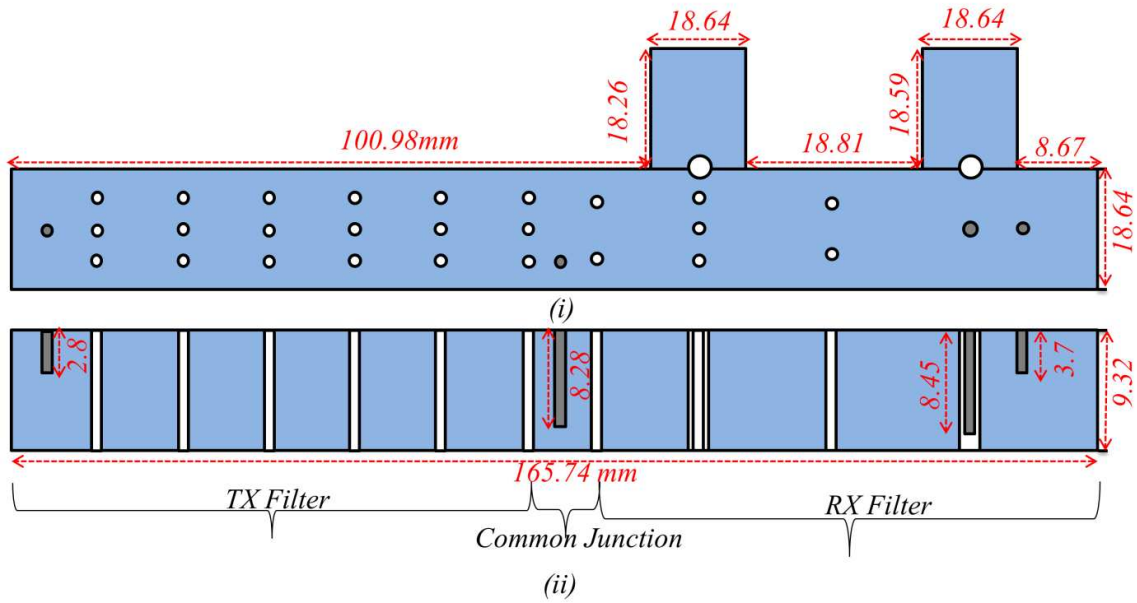


Figure 13. Ceramic waveguide diplexer layout (i) Top view (ii) Side view

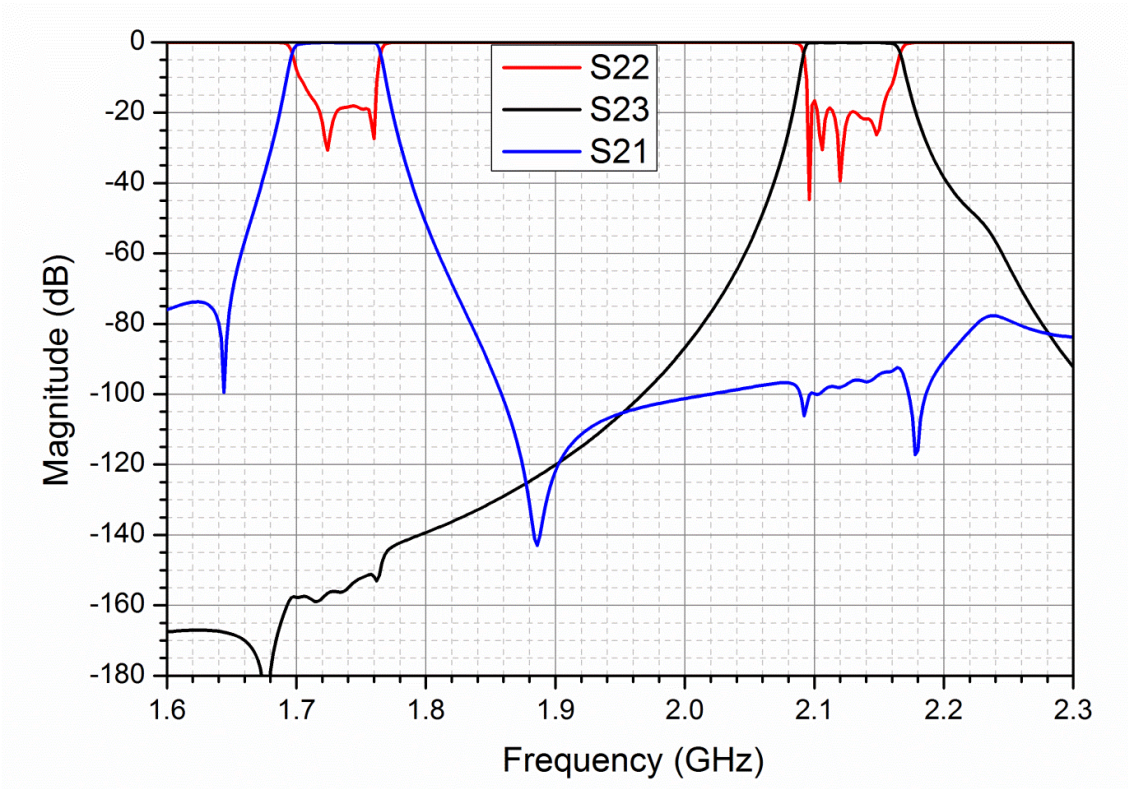


Figure 14. Simulated response of ceramic rectangular waveguide diplexer (HFSS™)

7. Practical Issues

Practical issues for fabrication are; the ceramic material used was Barium titanate with $\epsilon_r = 45$ and $\tan\delta = 0.00004$ for chebyshev filter and $\epsilon_r = 43$ and $\tan\delta = 0.00004$ for rest of the designs. The ceramic was fired and pressed and details were added by machining. The surface finish was $0.5\mu\text{m}$. The metallic coating was a silver loaded ink which was sprayed on to the ceramic; it had a conductivity of 4.4×10^7 s/m. The temperature coefficient of the ceramic was -4.5 ppm/ $^{\circ}\text{C}$.

8. Conclusion

The design of miniaturized integrated ceramic waveguide filters and a diplexer is presented in this paper. A monolithic six pole Chebyshev and a cross coupled generalized Chebyshev ceramic waveguide filter with tuning screws in it were designed and measured. The design of a monolithic integrated ceramic waveguide diplexer is also presented. Potential volume reduction of 50% is achieved as compared to conventional coaxial filters using high permittivity ceramics. Measured results for Chebyshev design are in good agreement with the simulated results with the one exception of pass band loss where leakage at input and output increases the pass band insertion loss. The measured results for generalized Chebyshev design are also well matched to the simulated results except the position of the lower side transmission zero which has moved closer to the passband. This is mainly due to mechanical tolerance of the blind hole in the ceramic providing stronger cross coupling than required.

9. Acknowledgement

The authors would like to thank the Royal Academy of Engineering and Radio Design Ltd for sponsorship of Prof. Ian Hunter and Sukkur IBA for sponsoring Yameen Sandhu.

10. References

- Atia, A. E., A. E. Williams, et al. (1974). "Narrow-band multiple-coupled cavity synthesis." IEEE Transactions on Circuits and Systems **21**(5): 649-655.
- Cameron, R. J. (1999). "General coupling matrix synthesis methods for Chebyshev filtering functions." IEEE Transactions on Microwave Theory and Techniques **47**(4): 433-442.
- Cameron, R. J. (2003). "Advanced coupling matrix synthesis techniques for microwave filters." IEEE Transactions on Microwave Theory and Techniques **51**(1): 1-10.

- Cohn, S. B. (1968). "Microwave Bandpass Filters Containing High-Q Dielectric Resonators." IEEE Transactions on Microwave Theory and Techniques **16**(4): 218-227.
- Haine, J. L. and J. D. Rhodes (1977). "Direct Design Formulas for Asymmetric Bandpass Channel Diplexers." IEEE Transactions on Microwave Theory and Techniques **25**(10): 807-813.
- Helszajn, J. and I. o. E. Engineers (2000). Ridge Waveguides and Passive Microwave Components, Institution of Engineering and Technology.
- Hunter, I., Ed. (2001). Theory and design of microwave filters. London, The institute of electrical engineers.
- Kapilevich, B. Y. and Y. R. Trubekhin (1989). "Monolithic dielectric filters in integrated waveguide technology." International Journal of Electronics **66**(3): 449-456.
- Keam, R. B. and A. G. Williamson (1994). "Broadband design of coaxial line/rectangular waveguide probe transition." IEE Proceedings on Microwaves, Antennas and Propagation **141**(1): 53-58.
- Khalaj-Amirhosseini, B. H. G. a. M. (2008). "Compact band pass filters utilizing dielectric filled waveguides." Progress In Electromagnetics Research B **7**: 105-115.
- Kurzrok, R. M. (1966). "General Four-Resonator Filters at Microwave Frequencies (Correspondence)." IEEE Transactions on Microwave Theory and Techniques **14**(6): 295-296.
- Kurzrok, R. M. (1966). "General Three-Resonator Filters in Waveguide." IEEE Transactions on Microwave Theory and Techniques **14**(1): 46-47.
- Levy, R. (1990). Synthesis of non-contiguous diplexers using broadband matching theory. IEE Colloquium on Microwave Filters and Multiplexers.
- Levy, R. and P. Petre (2001). "Design of CT and CQ filters using approximation and optimization." IEEE Transactions on Microwave Theory and Techniques **49**(12): 2350-2356.
- Levy, R., R. V. Snyder, et al. (2002). "Design of microwave filters." IEEE Transactions on Microwave Theory and Techniques **50**(3): 783-793.
- Liang, J. F., H. C. Chang, et al. (1992). "Coaxial probe modeling in waveguides and cavities." Microwave Theory and Techniques, IEEE Transactions on **40**(12): 2172-2180.
- Macchiarella, G. and S. Tamiazzo (2006). "Novel Approach to the Synthesis of Microwave Diplexers." IEEE Transactions on Microwave Theory and Techniques **54**(12): 4281-4290.
- Marcuvitz, N. and I. o. E. Engineers (1951). Waveguide Handbook, McGraw-Hill.
- Matthaei, G. L. (1980). Microwave filters, impedance-matching networks, and coupling structures, McGraw-Hill.
- Nishikawa, T. (1988). Microwave Ceramic Dielectrics and Their Applications. 18th European Microwave Conference, 1988.
- Rhodes, J. D. (1976). "Direct design of symmetrical interacting bandpass channel diplexers." IEE Journal on Microwaves, Optics and Acoustics **1**(1): 34-40.
- Rhodes, J. D. and R. J. Cameron (1980). "General Extracted Pole Synthesis Technique with Applications to Low-Loss TE₀₁₁ Mode Filters." IEEE Transactions on Microwave Theory and Techniques **28**(9): 1018-1028.
- Sanghoon, S. and S. Kanamaluru (2007). "Diplexer design using EM and circuit simulation techniques." IEEE Microwave Magazine **8**(2): 77-82.

- Sebastian, M. T. (2008). Dielectric materials for wireless communication. Elsevier Science Ltd, Elsevier Science Ltd.
- Sorrentino, R., L. Pelliccia, et al. (2011). Recent progress in miniaturized and reconfigurable filters for advanced communications and space applications. Microwaves, Radar and Remote Sensing Symposium (MRRS), 2011.
- Thomas, J. B. (2003). "Cross-coupling in coaxial cavity filters - a tutorial overview." IEEE Transactions on Microwave Theory and Techniques **51**(4): 1368-1376.
- Wolansky, D., J. Vorek, et al. (2010). Virtual prototyping of diplexers by using CST Studio. 15th International Conference on Microwave Techniques (COMITE), 2010